NASA Technical Memorandum 102589

A Method for the Reduction of Aerodynamic Drag of Road Vehicles

Bandu N. Pamadi,
Larry W. Taylor, and
Terrance O. Leary

(NASA-TM-102589) A METHOD FOR THE REDUCTION OF AERODYNAMIC DRAG OF ROAD VEHICLES (NASA) 25 p   CSCL 01A

N90-27050

Unclas
G3/02 0302683

January 1990

ABSTRACT

A method is proposed for the reduction of the aerodynamic drag of bluff bodies, particularly for application to road transport vehicles. This technique consists of installation of panels on the forward surface of the vehicle facing the airstream. With the help of road tests, it has been demonstrated that the attachment of proposed panels can reduce aerodynamic drag of road vehicles and result in significant fuel cost savings and conservation of energy resources.

Nomenclature

A,B   coefficients as defined in equation (2)

b_o width of the model

C_p pressure coefficient $= \dfrac{p - p_\infty}{\frac{1}{2} \rho_\infty V_\infty^2}$

C_D drag coefficient

C_{Do} drag coefficient of the basic model (no panels)

F_o frictional resistance $= \mu W$

g   acceleration due to gravity

h   height of the panel

J   cost function as defined in equation (3)

p   pressure

P_s percentage power/gas saving

r   distance measured along the bottom surface from corner to panel location as shown in figure 2.

S   frontal area of the vehicle

R_e Reynolds number based on width

V   velocity

W   vehicle weight

θ   the angle measured counter-clockwise to a given point on the model surface from the freestream direction as shown in figure 7

μ   coefficient of friction

Suffix

∞   freestream

INTRODUCTION

The drag of bluff bodies consists mainly of pressure drag, skin friction forming an insignificant part of the total drag. The flow field of bluff bodies is usually characterized by large wake and periodic vortex shedding. This is especially true of noncircular cylinders with sharp windward corners operating at low or moderate Reynolds numbers. The drag force associated with such flow pattern is very high (C_D=2.0). The existence of such flow patterns over the road transport vehicles can lead to substantial expenditure of fuel to overcome the vehicle aerodynamic drag.

The Reynolds number associated with small and medium size road vehicles usually falls in the subcritical range (up to 2 million). Therefore, the study of the flow field and drag coefficient of bluff bodies at subcritical Reynolds numbers is of great interest. The present investigation mainly applies to this range of Reynolds numbers.

One of the popular methods of reducing the aerodynamic drag of non-circular bluff bodies at subcritical Reynolds numbers is the rounding of sharp corners (ref. 1, 2). However, the maximum reductions achievable by the corner rounding technique appear to be limited to 50 percent. In reference 3, a method is proposed which is capable of achieving substantially higher aerodynamic drag reduction of bluff bodies compared to the corner rounding approach. This consists of installation of panels on the forward surface of the body facing the airstream. The panels are thin rigid flat plates. In the following, a brief description of this method of reference 3 which was developed through two-dimensional wind and water tunnel tests on a typical noncircular section (fig. 1) is presented. The application of this method to two road transport vehicles is discussed through actual road tests on a medium size van (fig. 2) and a passenger car (fig. 3).

DRAG REDUCTION METHOD

Two-Dimensional Tests

The geometry of the model tested in reference 3 is shown in figure 1. Panels (strakes) of various sizes (h/b_o = 0.1, 0.2, and 0.3) were employed and their location on the windward face was varied systematically (r/b_o = 0 to 0.5). Detailed pressure measurements were performed in a 61 cm × 61 cm (2ft × 2ft) low-speed wind tunnel having a maximum velocity of 35 m/s (115 ft/sec). Some water tunnel flow visualization tests (Reynolds number = 6000) were also carried out to aid in understanding and interpretating of wind tunnel test data. The pressure test Reynolds number was in the range of 0.6 to 2.0×10^6 (subcritical). Measured surface pressures were integrated to obtain drag coefficients. Additional information on the pressure and flow visualization tests is available in reference 3.

The important results of reference 3 are presented in figures 4 thru 6. Here, C_D and C_{Do} are respectively the drag coefficients of the model with and without the panels. The basic model (without the panels) has a drag coefficient of 2.23 which agrees well with the value given by Jorgensen (ref. 2) for a similar shape.

3

The effect of panels on C_D is quite interesting. Both the panel height and location, particularly the latter, have a strong influence on the drag coefficient. For all the locations of the panels, other than at the corners ($r=0$), the drag coefficient with panels was always less than that of the basic model. As seen in figure 4, large reductions in drag coefficient occur when the panels are located at $r/b_o = 0.2$ and of the configurations tested, maximum reduction occurs for a panel height of $h/b_o = 0.3$. For this case, $C_D/C_{Do} = 0.185$ or a drag reduction of 81.5 percent which is much higher than the maximum of 50 percent said to be possible by the corner rounding technique (ref. 2).

Mechanism of Drag Reduction

a. Streamlining Effect: The panels produce a streamlining effect over the body. The width of the wake is reduced and vortex shedding is greatly suppressed. As speculated in reference 3, a reason for this phenomenon is the transition in the flow consequent to the separation at the strakes and a smooth reattachment to the body surface as noticed in the flow visualization photograph of figure 5. The reattached flow sticks to the body surface to more extent before eventually separating, thereby leading to substantial base pressure recovery as noted in figure 6. The steep pressure rise (fig. 6) prior to flow separation is characteristic of turbulent boundary layer separation. This kind of flow pattern with drag coefficient well below the subcritical value is typical of bluff body flow at supercritical Reynolds numbers.

For the subject noncircular section, the critical Reynolds number is in excess of 4×10^6 (ref. 2). Thus, the panels have produced the supercritical flow conditions with attendant drag reduction at subcritical free stream Reynolds numbers.

b. Generation of Thrust on the Forward Face: Generally, for a body facing the air stream, positive pressures are formed on the forward surface. However, with the panels on, these positive pressures are confined to the region bounded by the panels. Between the corners and the panels suction bubbles are formed which give rise to negative pressures on parts of the windward face and contribute significantly to drag reduction as shown schematically in figure 7.

APPLICATION TO ROAD TRANSPORT VEHICLES

The above drag reduction technique was applied to road transport vehicles by way of exploratory road tests on the following vehicles: (1) medium capacity van (fig. 2), and (2) medium size passenger car (fig. 3). The following panel configurations were tested.

Van:

Configuration 1: Panels on three sides (A, B, and C) as shown in figure 8. This configuration is an attempt to capture the negative pressures on all three sides of the frontal surface of the vehicle.

Configuration 2: Top panel (C) of the configuration 1 is deleted. Only side panels (A and B) are retained.

<u>Configuration 3</u>: Side panels (A and B) of configuration 2 extended up to the top.

For configurations 1 thru 3, the nondimensional height (h/b_0) of the panels was approximately equal to 0.133. Actually panels of bigger size (h/b_0=0.3) as indicated by two dimensional tests were installed initially but did not perform better.

<u>Configuration 4</u>: Same as in configuration 3 but panel nondimensional height reduced by half to h/b_0 = 0.067.

For all the above four configurations, the panels were located at r/b_0 = 0.2.

Passenger Car

Only one panel configuration (h/b_0 = 0.098, r/b_0 = 0.20) as shown in figure 9 was tested.

ROAD TESTS

These tests consisted of (a) deceleration tests, and (b) flow visualization tests.

Deceleration Tests

The vehicle deceleration (dV/dt) is given by the following equation,

$$\frac{dV}{dt} = - \frac{g}{W} \left(F_0 + \frac{1}{2} \rho V^2 SC_D \right), \tag{1}$$

where

W = gross weight

V = speed

$F_0 = \mu W$

μ = coefficient of friction

ρ = density of air

S = frontal area

C_D = aerodynamic drag coefficient.

The approach taken here is to measure the actual deceleration of the vehicle at various speeds and then apply the least square technique to determine F_0 and C_D. Rewrite the equation (1) as follows:

$$\frac{dV}{dt} = A + B V^2 \tag{2}$$

5

where

$$A = -F_o \, g/W, \qquad B = -S \, C_D \, g \, \rho/2W. \tag{3}$$

Next, define the least square cost function as

$$J = \sum_{i=1}^{N} \left[\frac{dV_i}{dt} - (A + B \, V_i^2) \right]^2 \tag{4}$$

where

$i = 1$ to N are the number of road test data points

V_i = measured speed

$\dfrac{dV_i}{dt}$ = measured deceleration

Next, for minimization of J, w.r.t. A and B, differentiate J with respect to A and B and equate the resulting expression to zero

$$\partial J/\partial A = -2 \sum_{i=1}^{N} \left[\frac{dV_i}{dt} - (A + B \, V_i^2) \right] = 0 \tag{5}$$

and

$$\partial J/\partial B = -2 \sum_{i=1}^{N} \left[\frac{dV_i}{dt} - (A + B V_i^2) \right] V_i^2 = 0 \tag{6}$$

The equations (5) and (6) lead to the following equation in the matrix form to determine the unknowns A and B.

$$\begin{bmatrix} A \\ \\ B \end{bmatrix} = \begin{bmatrix} N & \Sigma V_i^2 \\ \\ \Sigma V_i^2 & \Sigma V_i^4 \end{bmatrix}^{-1} \begin{bmatrix} \Sigma dV_i/dt \\ \\ \Sigma V_i^2 \, dV_i/dt \end{bmatrix} \tag{7}$$

The ground resistance and drag coefficient C_D can then be obtained as,

$$F = - \frac{AW}{g} \quad \text{and} \quad C_D = -2 \, WB/\rho \, gS. \tag{8}$$

6

Procedure

The test vehicles were weighed with known quantities of gasoline. The odometer of both vehicles were carefully calibrated. The deceleration was determined by noting the time for the speed to drop by 10 mph from a selected initial value. An accurate ($\pm$ 0.01 sec) digital stop watch was used for measurement of corresponding time intervals. The average deceleration was obtained by the following relation

$$\frac{dV}{dt} = \frac{V_o - V_f}{\Delta t} \tag{9}$$

where

V_o = initial speed

V_f = final speed

Δt = time interval for speed to drop from V_o to V_f

For the van, selected initial speeds (V_o) ranged up to 80 mph. However, for the passenger car, the test speeds were limited to the range of 60 mph. For each speed range more than 15 values of deceleration were recorded.

Flow Visualization Tests

The purpose of these tests was to explore the effect of panels on the flow pattern around the vehicle. These tests were conducted only on the van. Tufts of 1 to 2 inches in length were cut out of cotton yarn and were attached to the vehicle by cellophane tape. Since the flow pattern is normally symmetrical, tufts were fixed to only one side of the vehicle. Extensive flow visualization photographs were taken at various speeds.

RESULTS

The results of road tests are presented in figures 10 thru 13. Photograph of the test vehicle with tufts is shown in figure 14. Based on the flow visualization photographs, schematic sketches of the flow around the vehicle are drawn as shown in figure 15.

Van: From figure 10, we notice that the drag coefficient of the basic vehicle (no panels) decreases rapidly in the neighborhood of 25 mph and subsequently falls at a much slower rate. Therefore, it appears that the test Reynolds number at higher speeds is approaching the critical value.

The installation of panels leads to substantial drag reduction. Of the four-panel configurations tested, the panel configuration no. 4 gave the best results. For this configuration, the maximum reduction of 27 percent in aerodynamic drag and attendant fuel/power reduction of 18 percent occur around 40 mph (fig. 11). At the normal freeway driving speed of 55 mph, the corresponding values are respectively 8.5 and 6.5 percent.

Passenger Car: From figure 12 and 13(a) we observe that at speeds below 30 mph (44ft/sec), there is a substantial drag reduction to the extent of 60 percent but falls to 6.5 percent at 55 mph. As was the case for the van, the fuel saving is approximately 6 percent (fig. 13(b)) at 55 mph for the passenger car. The panel configuration is also very similar to the configuration 4 on the van.

Mechanism of Drag Reduction

The tufted vehicle (fig. 14) was driven at various speeds to obtain flow visualization photographs. From a study of these flow visualization photographs, it was found that over the basic vehicle (fig. 15(a)) the flow separates around the corner and reattaches downstream of the side window. With the installation of panels the reattachment point comes close to the corners as shown in figure 15(b). Thus the panels, as noted earlier for the two-dimensional flow over noncircular cylinder, have produced a smooth reattachment of the separated flow very close to the corners. This smooth reattachment, coupled with suction on the forward face as speculated in two-dimensional tests is believed to give the observed drag reductions. However, actual measurement of this suction effect was not performed for the test vehicles. The magnitude of drag reduction is much smaller on road vehicles because of three-dimensional geometry. The associated flow field may not support large suction pressures on the frontal face as observed for two-dimensional, noncircular section models.

CONCLUDING REMARKS

The technique of installing panels on the forward part of the non-circular, sharp-edged bluff cylinder facing the air stream gives a substantial drag reduction compared to the familiar corner rounding or other streamlining methods and holds promise for application to three-dimensional bodies such as road vehicles.

This technique is applied to two typical road transport vehicles a medium size van and a passenger car. At 55 mph, the percentage drag reductions were 8.5 and 6.5 for the van and car, respectively, indicating a 6 percent fuel savings in both cases.

The panels are easy to install and can be made out of transparent material so that they do not obstruct the driver's vision. Also, they can be made retractable and deployed in the speed range where they are most effective.

REFERENCES

1. Hoerner, S. F.: <u>Fluid Dynamic Drag</u>, Brick Town, New Jersey, 1965.

2. Jorgensen, L. H. and Brownson, J. J.: "Effect of Reynolds Number and Body Corner Radius on Aerodynamic Characteristics of a Space Shuttle-type Vehicle at Subsonic Mach Numbers." NASA TN D-6615, 1972.

3. Pamadi, B. N., Pereira, C., and Gowda, B.H.L.: "Drag Reduction by Strakes of NonCircular Cylinders." <u>AIAA Journal</u>, Vol. 26, March 1988, pp. 292-299.
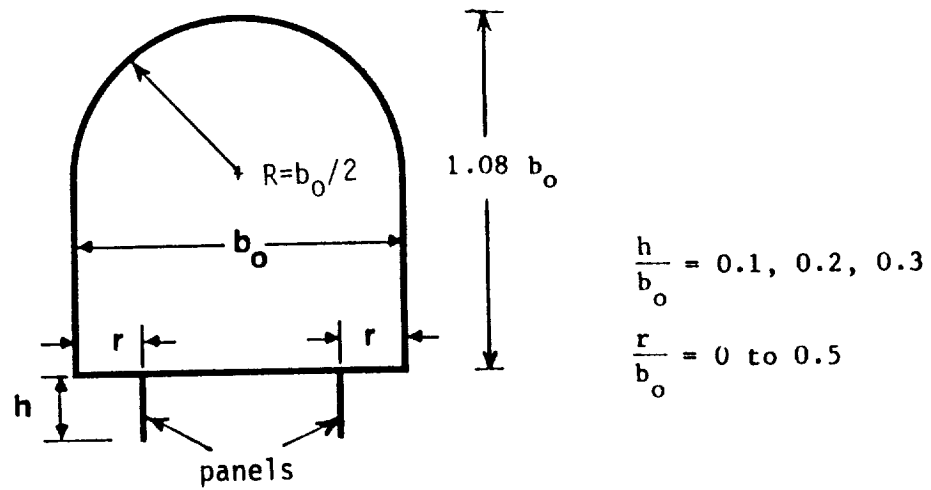
The figure shows a model cross-section with a semicircular top of radius $R = b_0/2$ and an overall height of $1.08\ b_0$. The width across is b_0. At the bottom corners are dimensions r on each side, with height h below, pointing to "panels."

$$\frac{h}{b_0} = 0.1,\ 0.2,\ 0.3$$

$$\frac{r}{b_0} = 0 \text{ to } 0.5$$

Figure 1. Model Geometry and Panel Configurations.

Figure 2. Photograph of Test Van with Panels

Figure 3. Photograph of Test Car with Panels

11
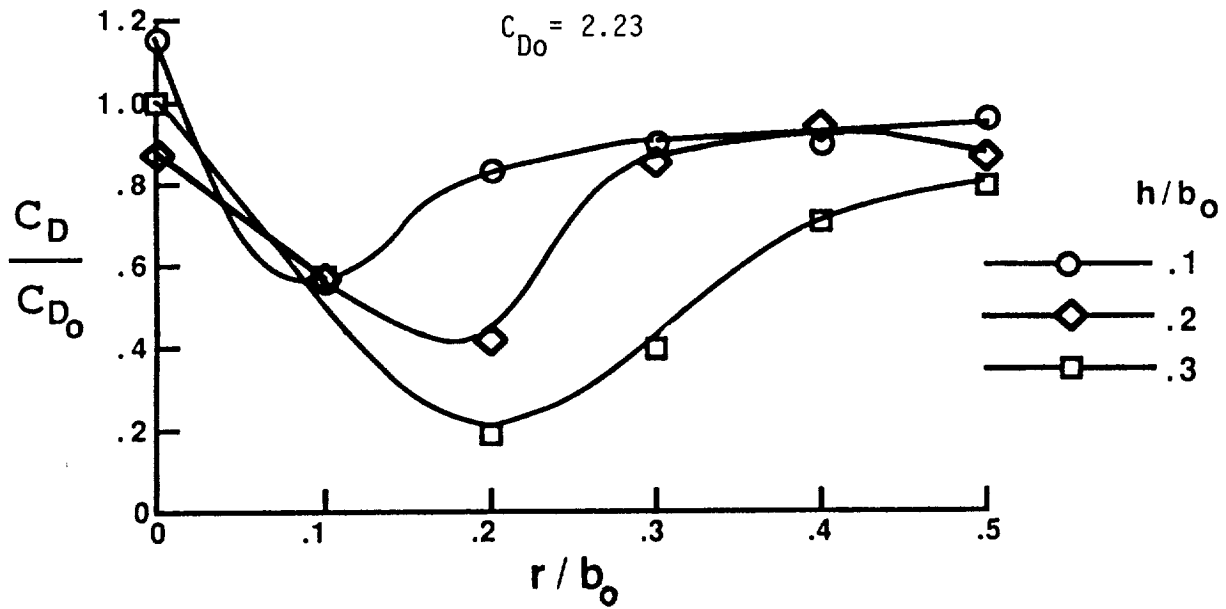
Figure 4. Effect of Panels on Drag Coefficient
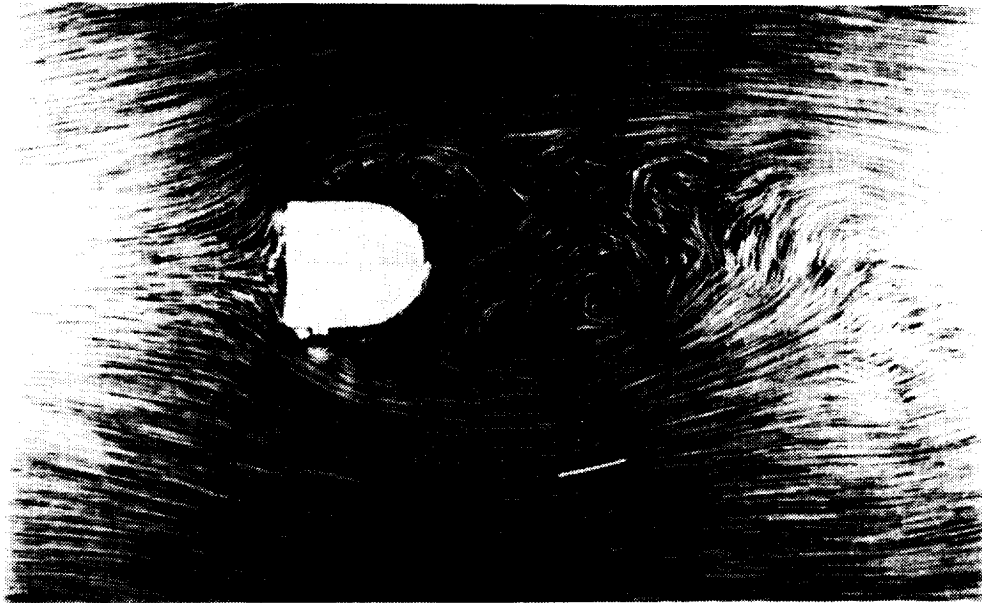
(a) Basic Model
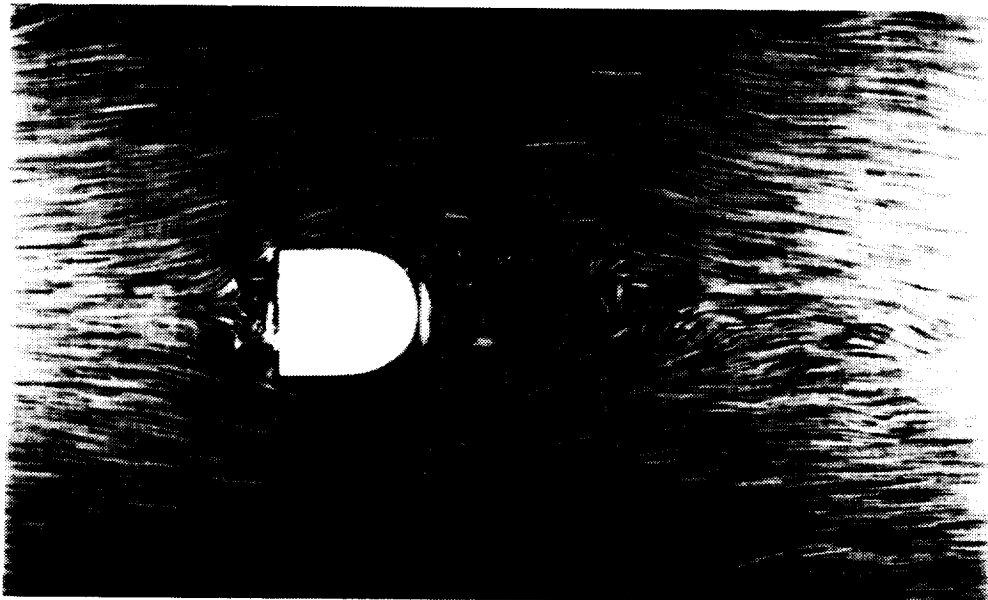
(b) Panel Configuration $h/b_o = 0.3$, $r/b_o = 0.2$

Figure 5. Water Tunnel Flow Visualization Photographs

13
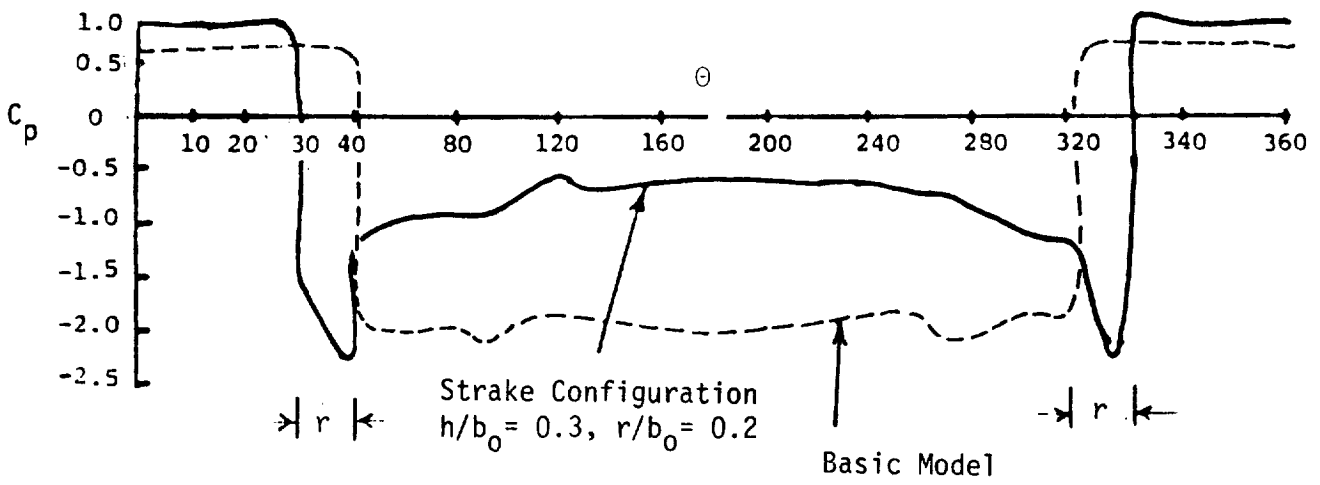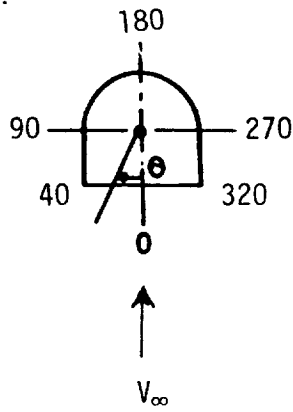
Figure 6. Pressure Distributions

ΔF - Thrust Force

ΔD - Drag Force
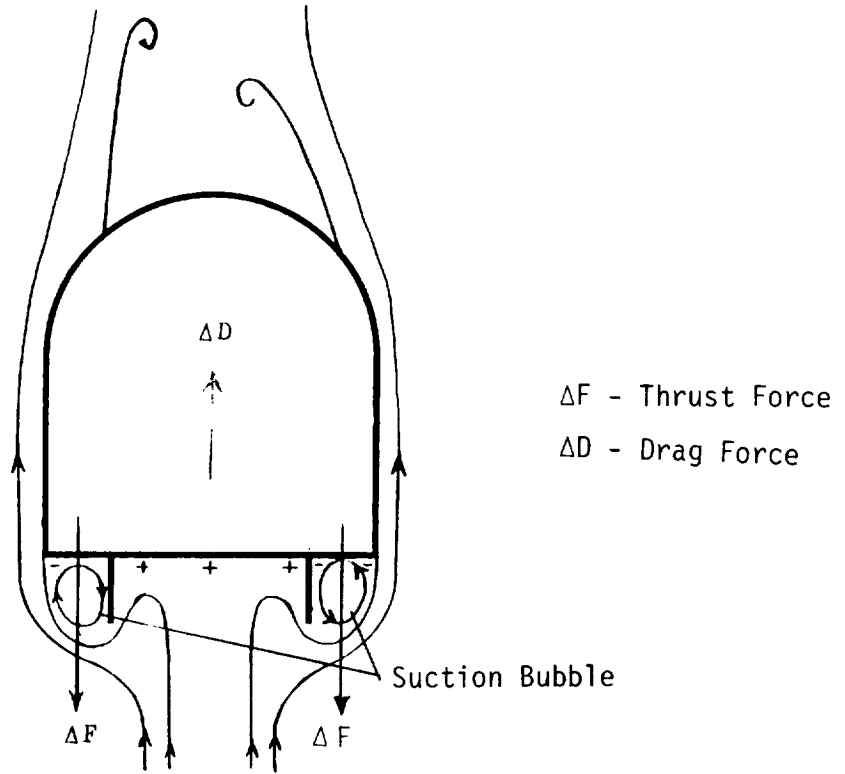
Figure 7.   Schematic Flow Patterns
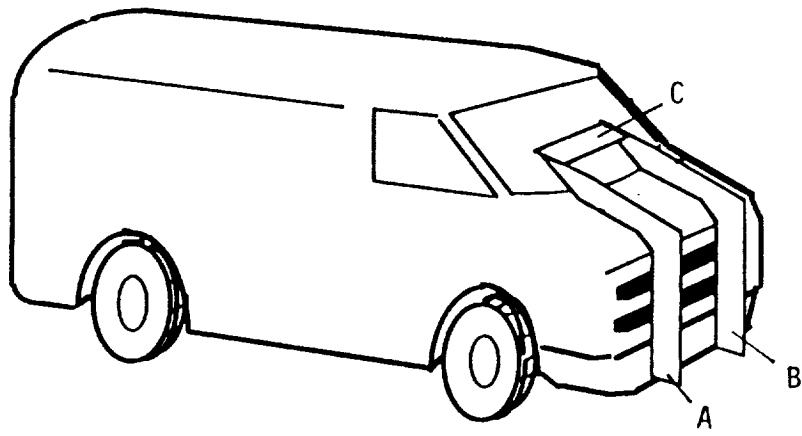
Configuration 1
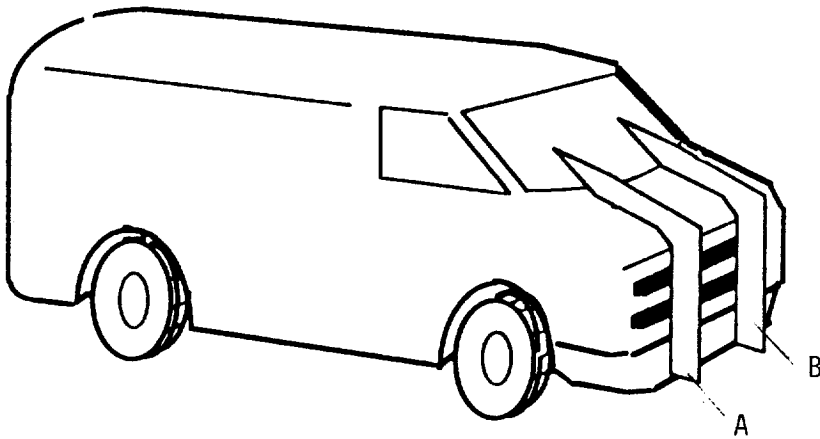
Configuration 2
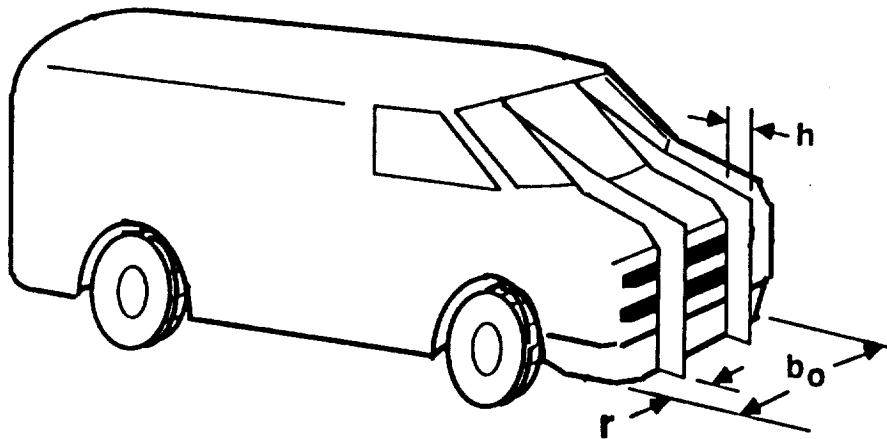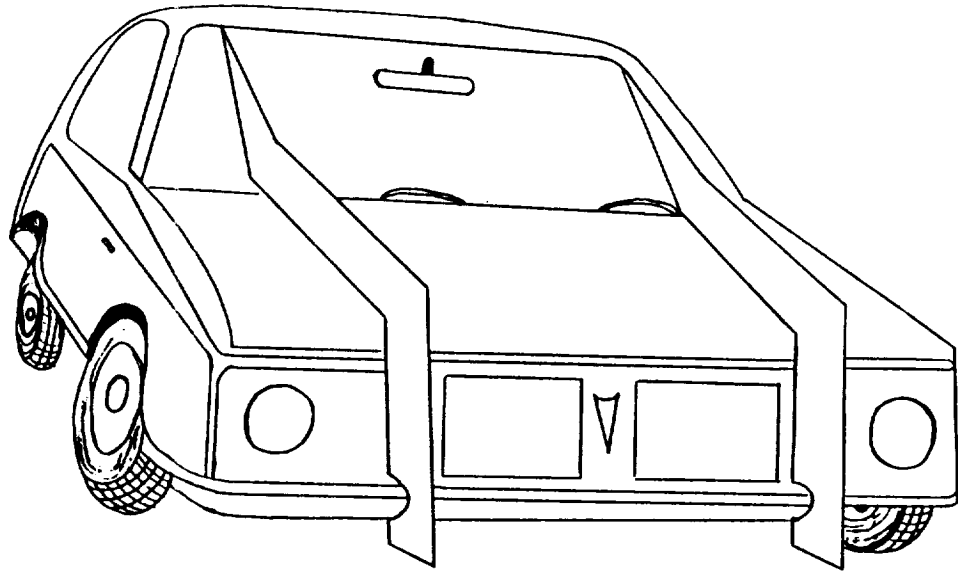

Configurations 3 and 4

Figure 8. Panel Configurations (Van)
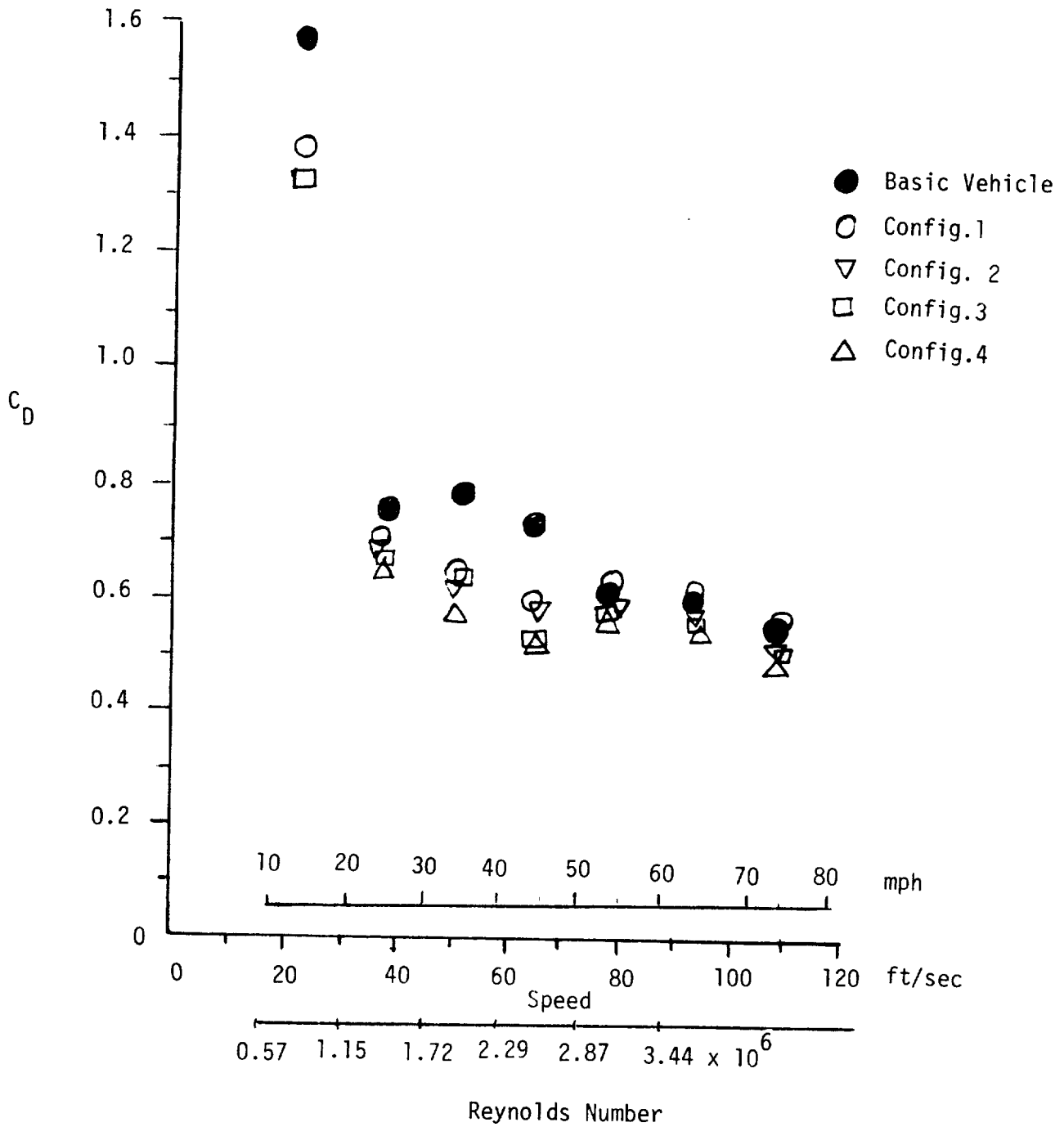
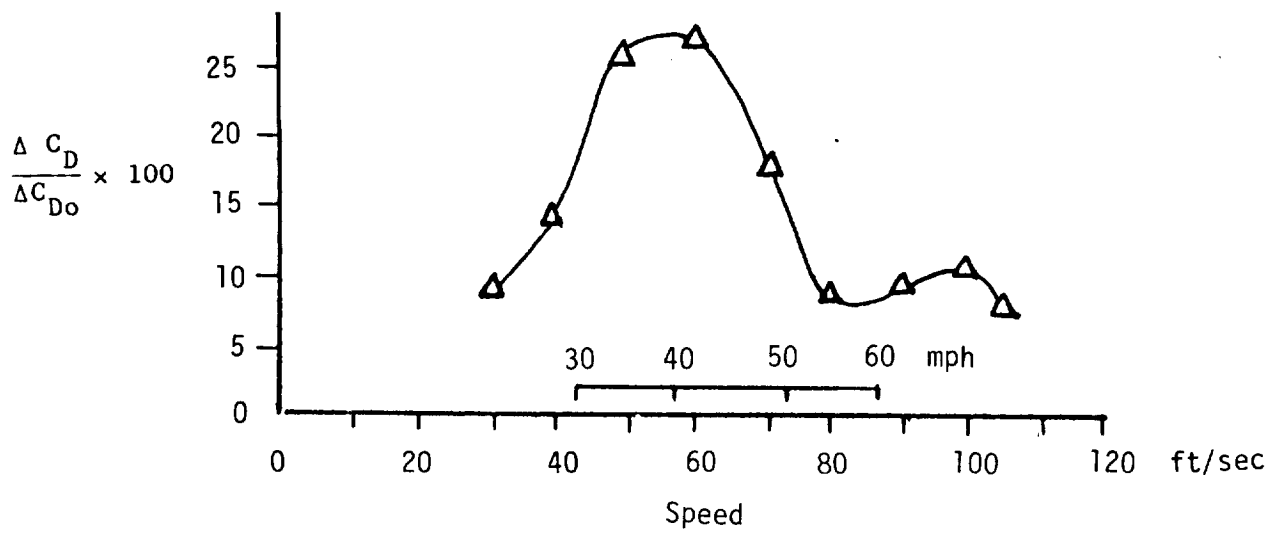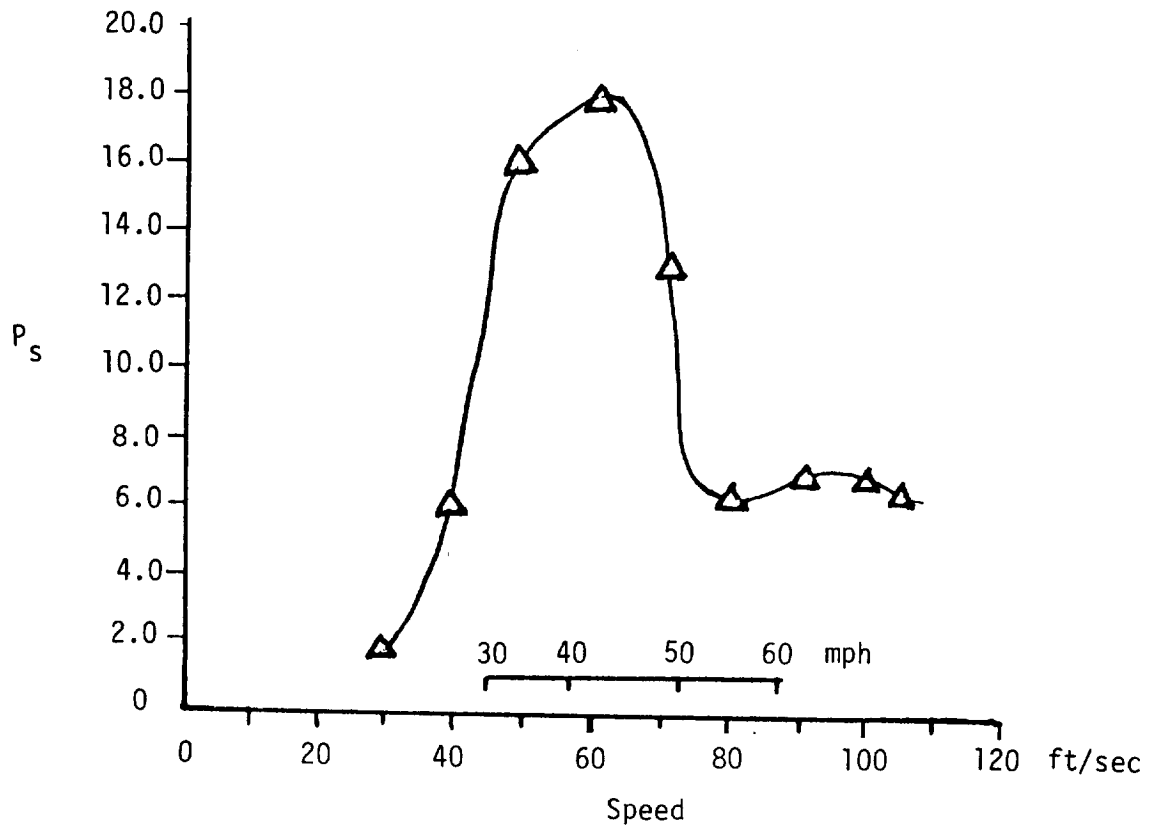Figure 9. Panel Configuration (Passenger Car)

C_D

1.6

1.4

1.2

1.0

0.8

0.6

0.4

0.2

0

● Basic Vehicle
○ Config.1
▽ Config. 2
□ Config.3
△ Config.4

10 20 30 40 50 60 70 80 mph

0   20   40   60   80   100   120 ft/sec

Speed

0.57 1.15 1.72 2.29 2.87 3.44 x 10^6

Reynolds Number

Figure 10. Variation of Drag Coefficient with Speed (Van)

(a) Percentage Drag Reduction

(b) Percentage Power/gas Saving

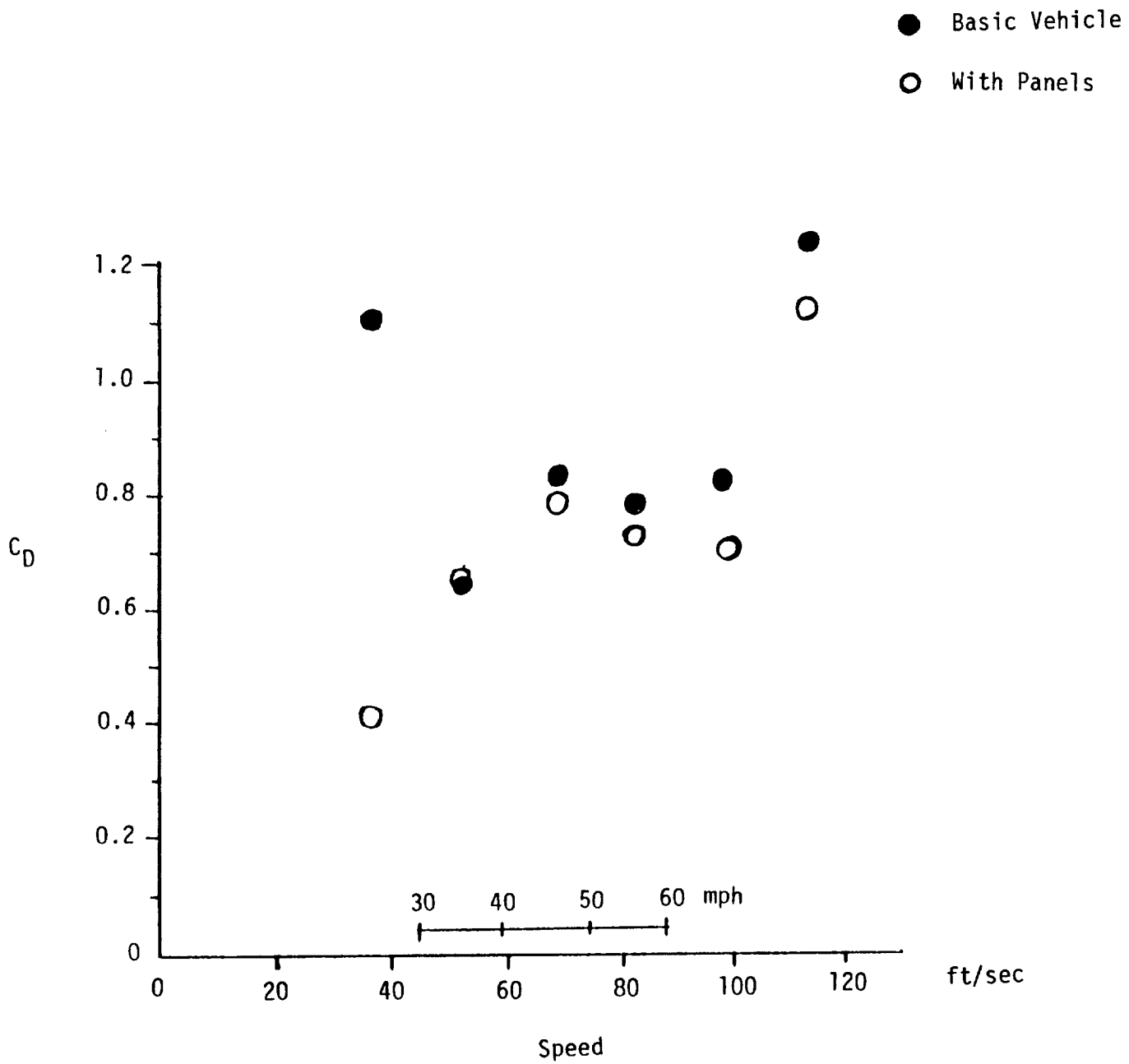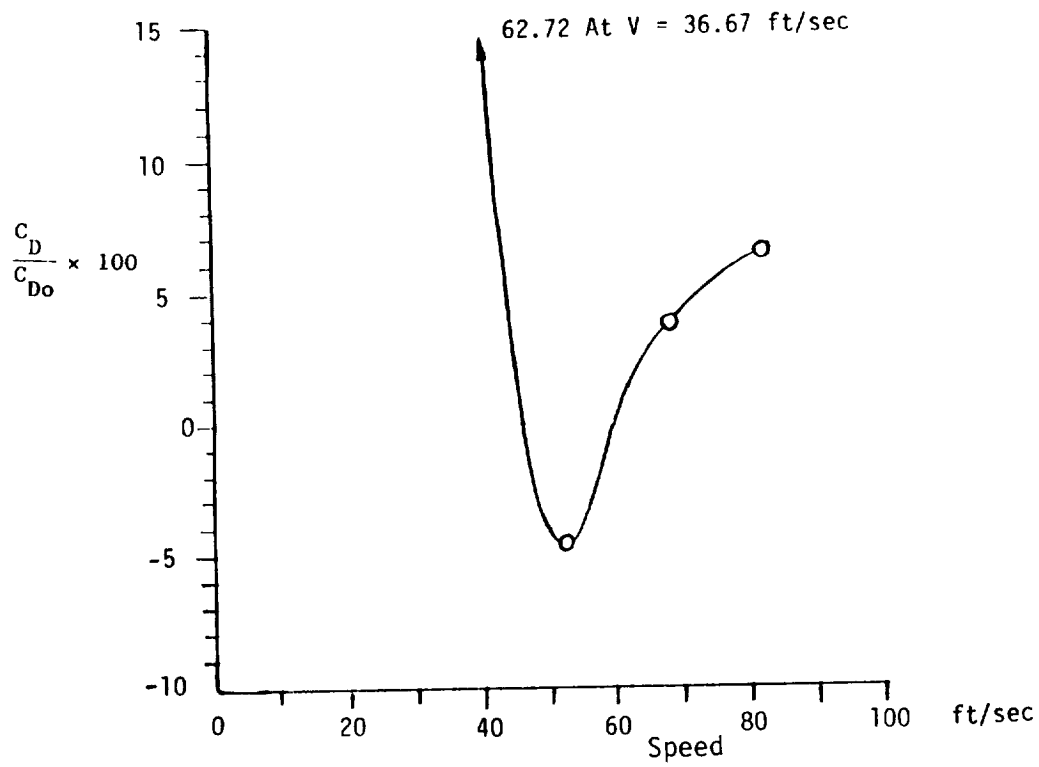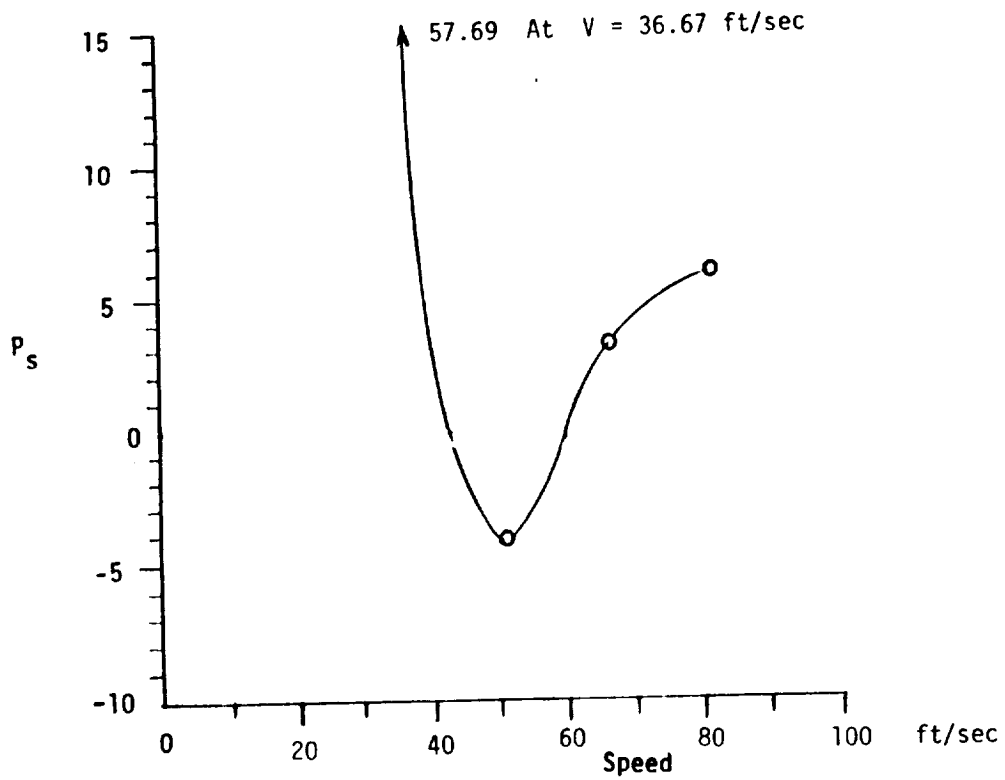Figure 11. Test Results (Van, Panel Configuration No. 4)

Figure 12. Variation of Drag Coefficient (Passenger Car)

62.72 At V = 36.67 ft/sec

(a) Percentage Drag Reduction

57.69 At V = 36.67 ft/sec

(b) Percentage Power/gas Saving

Figure 13. Test Results (Passenger Car)

21

Figure 14. Photograph of Tufted Test Vehicle (Van)

Attached Flow

Reattachment Line

(a) Basic Vehicle
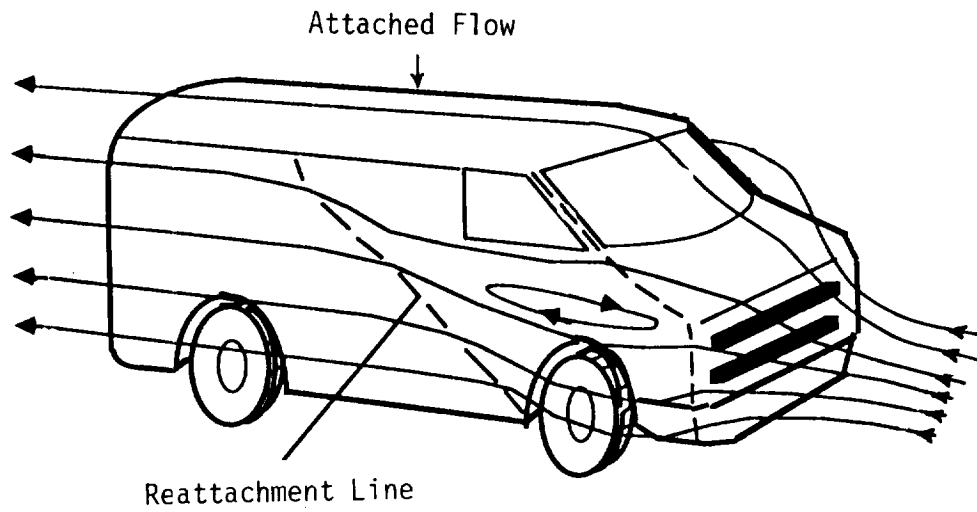
Flow Reattachment Line
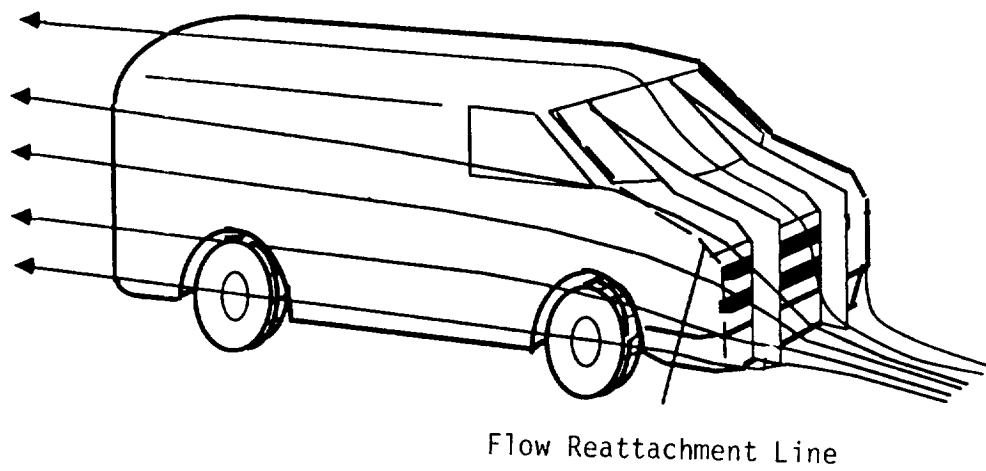
(b) Panel Configuration 4

Figure 15. Sketches of Flow Pattern (Van)

1. Report No. NASA TM-102589	2. Government Accession No.	3. Recipient's Catalog No.
4. Title and Subtitle A Method for the Reduction of Aerodynamic Drag of Road Vehicles		5. Report Date January 1990
		6. Performing Organization Code
7. Author(s) B. N. Pamadi*, L. W. Taylor, and T. O. Leary#		8. Performing Organization Report No.
		10. Work Unit No. 506-46-21-01
9. Performing Organization Name and Address NASA Langley Research Center Hampton, VA 23665-5225		
		11. Contract or Grant No.
12. Sponsoring Agency Name and Address National Aeronautics and Space Administration Washington, DC 20546-0001		13. Type of Report and Period Covered Technical Memorandum
		14. Sponsoring Agency Code

15. Supplementary Notes

* Senior Research Scientist, Vigyan Research Associates, Inc., 30 Research Dr., Hampton, VA 23665
# Graduate Student, George Washington University - Joint Institute for Advancement of Flight Sciences, MS 269, Hampton, VA 23665

16. Abstract

A method is proposed for the reduction of the aerodynamic drag of bluff bodies, particularly for application to road transport vehicles. This technique consists of installation of panels on the forward surface of the vehicle facing the airstream. With the help of road tests, it has been demonstrated that the attachment of proposed panels can reduce aerodynamic drag of road vehicles and result in significant fuel cost savings and conservation of energy resources.

17. Key Words (Suggested by Author(s)) Drag Reduction Application to Road Transport Vehicles	18. Distribution Statement Unclassified - Unlimited Subject Category 02

19. Security Classif. (of this report) Unclassified	20. Security Classif. (of this page) Unclassified	21. No. of pages 24	22. Price A03